Alexandria Engineering Journal (2022) 61, 10791–10803

HOSTED BY

Alexandria University

Alexandria Engineering Journal

www.elsevier.com/locate/aej
www.sciencedirect.com

A novel wide dual band circularly polarized dielectric resonator antenna for milli meter wave 5G applications

Abinash Gaya [a], Mohd. Haizal Jamaluddin [a,*], Bader Alali [b,c], Ayman A. Althuwayb [c]

[a] Wireless Communication Center, Universiti Teknologi Malaysia, Johor 81310, Malaysia
[b] Center for Wireless Communications, Institute of Electronics, Communications and Information Technology, Queens University Belfast, Belfast, Northern Ireland, UK
[c] Department of Electrical Engineering, Jouf University, Sakaka 72388, Aljouf, Saudi Arabia

Received 30 November 2021; revised 14 March 2022; accepted 11 April 2022
Available online 20 April 2022

KEYWORDS

Dielectric Resonator Antenna;
Milli meter wave;
5G. Dual Band;
Circularly Polarized

Abstract A novel singly fed Dielectric Resonator Antenna (DRA) is proposed here for milli meter wave 5G (Fifth Generation) frequency band applications. The DRA has achieved wide dual bandwidth with circular polarization at the defined 5G frequency bands. The resonances of this dual band antenna occur at 22.06 GHz, 24.5 GHz and 29.84 GHz. The percentage bandwidth $|S11| < -10$ dB of 26.3% is achieved at the first band (19.52–26.36 GHz) and 7.69% at the second band $|S11| < -10$ dB (28.26–30.26 GHz). Both the achieved bands here are covered under the Band 30 GHz category of 5G frequency spectrum. Compared to the conventional rectangular DRA, a novel trapezoidal shaped DRA is designed here which is fed by a microstrip line with characteristics impedance of 50 Ohm. The defined electrical dimensions of the DRA are $0.25\lambda_0 \times 0.29\lambda_0 \times 0.22\lambda_0$ considering 26 GHz as its resonating frequency. The DRA is placed over a Rogers substrate with dimensions $0.5\lambda_0 \times 0.5\lambda_0 \times 0.1\lambda_0$ and permittivity of 2.2. The DRA is circularly polarized and has a 3-dB axial ratio bandwidth of 5.23%. The DRA has achieved a gain value of 3.28 dB. Milli meter wave communications require wideband antennas with circular polarization features to support high throughput communication channels. This singly fed DRA has achieved wide dual bandwidth with circular polarization and is more suitable for indoor 5G small cell applications.

1. Introduction

Milli meter wave communications have been under tremendous focus for implementation of 5G (Fifth Generation) applications. 5G antenna systems requires wideband antennas which can enhance the throughput of the channel. Dielectric resonator antennas (DRA) have been preferred compared to

* Corresponding author.
E-mail address: haizal@fke.utm.my (M.H. Jamaluddin).
Peer review under responsibility of Faculty of Engineering, Alexandria University.

https://doi.org/10.1016/j.aej.2022.04.025

other metallic antennas at milli meter wave communications because of its small size, higher radiation efficiency and easy coupling to transmission lines, and also for obtaining different radiation characteristics under different excited modes [1]. In comparison with planar antennas, a DRA is more flexible and adaptable due to its characteristics of diversity in structure and materials permittivity. Antennas with wider bandwidth and circular polarization can further enhance the channel capacity with better coverage for both indoor and outdoor cells. In milli meter wave antenna system multiple feeding techniques are used to generate such circular polarization in the desired antenna systems. Different shapes of Dielectric Resonators are more conveniently used at milli meter wave frequency bands in the last decade. However, rectangular shaped DRA's offer practical advantages over cylindrical and spherical shapes of dielectric resonators. As, the mode degeneracy can be avoided in the case of rectangular DRA's by sensibly choosing the three dimensions of the resonator along three coordinate axes. Further, for a give resonant frequency, two aspect ratios of a rectangular DRA (height/length and width/length) can be chosen independently [1,2]. The length and width to height ratio of a rectangular DRA gives a better aspect ratio and more flexibility in terms of bandwidth optimization [3]. The design of Dielectric Resonator antennas can be characterized using the information on radiated fields, resonant frequency, bandwidth, the radiation quality(Q-factor), and the field distribution inside the resonator [4]. Different shapes of DRA are shown here designed at milli meter wave frequency bands as cylindrical [5], tetrahedron [6], rectangular [7], triangular [8], stacked [9]. The fundamental mode of excitation in DRA depends on its feeding schemes and at the source point or feeding point. Several feeding schemes like microstrip line, aperture coupled [10], coaxial probe [11] are used to energize the DRA at milli meter wave frequency bands and as per the needs of users. DRA has been used as most suitable antenna for 5G milli meter wave frequency bands because of wide bandwidth and high efficiency. Fig. 1 shows the different shapes of DRA that are proposed before in the literature.

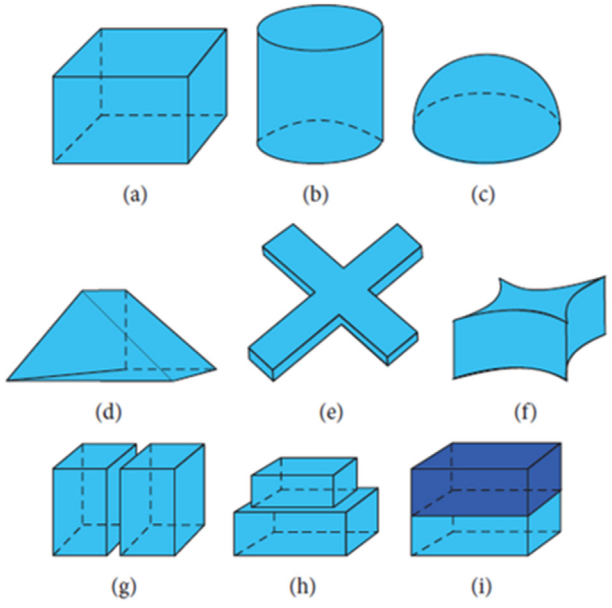

Fig. 1 Different shapes o DRA [12].

In this paper we propose this newly designed trapezoidal shaped DRA which is formed from the rectangular shaped DRA by means of edge angular cuts in the side arms. Here we have also compared the performance parameters as reflection coefficient, gain and axial ratio of both the rectangular and trapezoidal DRAs to examine its basic characteristics.

The antenna design calculations were done using MATLAB and simulation work were performed using Ansys HFSS (High Frequency Structure Simulator). Further the measurement of gain and radiation pattern were done inside the anechoic chamber using a 40 GHz horn antenna. All the boundary condition of perfect electric and magnetic field were followed with the mesh analysis in Ansys HFSS. During the process of fabrication an adhesive glue was used to fix the DRA on the substrate. The performance of this newly shaped trapezoidal DRA at milli meter wave frequency is compared with the previously designed dielectric resonators, which is mentioned in table at the end of this article. This singly fed DRA has many advantages of ultra-wide bandwidth and circular polarization at milli meter wave frequency compared to all previous work mentioned here. The signal to noise ratio performance can also be enhanced using wideband antennas with circularly polarization. Several DRA shapes have been proposed in the last decade, but here we are proposing a novel trapezoidal shaped DRA which has generated dual bandwidth with a microstrip line feed. The DRA shape is shown in Fig. 2, which is compared with a rectangular shaped DRA which we had used before. Here the broadside radiation of the antenna is at Phi = 0 and Theta = 0 which is more suitable for 5G indoor small cells. The details of design specifications and changes in resonators structure are shown in Section 3 of this article. The major contributions of this article are 1. A novel DRA is designed and proposed to be used at millimetre wave frequency band 2. The DRA has generated dual bandwidth at millimetre wave frequency band which can be used for 5G indoor applications. 3. The edge feed microstrip line to the DRA has generated circular polarization in the antenna. The edge feeding scheme is investigated at different feeding positions for generating circular polarization. The study of different shapes of DRA are analysed in the introduction. Section 2 of the article shows the novel unit cell design of the antenna, section 3 represents the mathematical analysis of the DRA. The parametric study and analysis is shown in section 4 of this article. The measured results are shown in section 5 of this article.

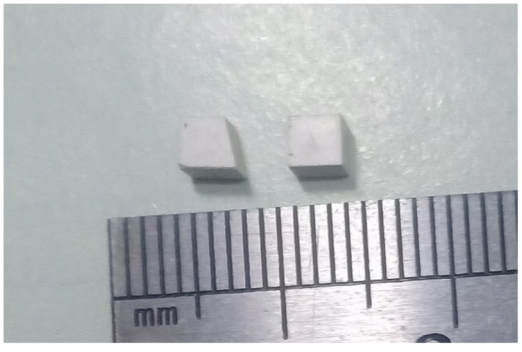

Fig. 2 Proposed DRA Shapes.

2. Antenna design and analysis

A ECCOS-TOCK Hik ceramic material based Dielectric Resonator Antenna with permittivity, εr = 10 and loss tangent 0.002 is used for a Roger RT/Duroid 5880 substrate with permittivity, εr = 2.2, loss tangent 0.0009, thickness 0.254 mm. The DRA dimensions and the substrate dimensions are calculated as per the resonating wavelength. The DRA is placed over the substrate with dimensions of 5.76 mm × 5.76 mm × 0.254 mm. The calculated resonating frequency here is 11.52 mm. The ceramic-based DRA has higher values of quality factor (Q-factor) which helps the DRA to achieve larger bandwidth at milli meter wave frequency bands [13]. The microstrip feed line is used to feed the DRA which is placed above to the substrate and a partial ground plane is used which is present at the other side of the substrate. The DRA design is shown in Fig. 3 (a) and the ground plane is shown in Fig. 3(c). The details of the DRA design parameters are shown in Table 1. This trapezoidal shaped DRA has been made from the rectangular DRA by few angular cut sections which has improved the bandwidth and gain of the singly fed DRA. These angular cut sides are optimized to achieve the maximum impedance bandwidth. The DRA positioning over the substrate has been done at x = 0, y = 0 and z = 0.254 mm which is the thickness of the substrate. The conditions of perfect electric and magnetic walls are applied here. The calculations of aspect ratio with respect to the permittivity of the ceramic material are shown in Table 2.

Fig. 3 shows the top view of the DRA with dimensions of microstrip feed line. The electric field distribution over the DRA is shown in Fig. 4(a) and (b) in XY plane and YZ plane respectively. The DRA designed here circularly polarized and it's marked in the Figs. 4 and 5. The surface current distribution over the partial ground plane is shown in Fig. 5.The mode excited in the DRA here TEX21 mode and has three resonances at |S11| < −10 dB generating dual band characteristics. The DRA is circularly polarized during the first resonance and is linearly polarized in second resonance. The input impedance of the antenna is matched with the characteristics impedance of 50 ohm and has reactance value near to zero. Microstrip line feed technique is most convenient is the rectangular DRA design as it enhances the radiation efficiency of the antenna with perfect input impedance matching [14]. It is also directly coupled to the DRA as the DRA is placed directly over the microstrip feed line containing an impedance match with the source connector at the edge of the substrate. The microstrip line feed in conventional designs generally given at the center of the DRA but here the position is optimized with the input impedance to achieve maximum impedance bandwidth. This wide bandwidth is achieved with high Q factor of the DRA as calculated as per the desired resonating frequency. The center frequency is shifted to lower frequency 26 GHz and above as per the impedance variation and transmission line match. The DRA under normal excitation and single mode acts as a magnetic dipole, as shown in Fig. 6. The electric field density in terms on intensity distribution is shown. The DRA field distribution depends on the feed point excitation and coupling to source connector and substrate thickness.

The aspect ratio calculations are shown in Table 2 with the calculated Q factor of the DRA. The permittivity values of the DRA is used to calculate the other antenna parameters as effective permittivity, and bandwidth [12]. For wideband antennas the permittivity of the DRA is chosen as 10 or above in milli meter wave frequencies.

3. Antenna design steps and mathematical analysis

The rectangular DRA has been used as most conventional shape DRA in all wireless applications but despite its good characteristic's there were chances to enhance its bandwidth and gain. So, this new shape was prepared by subtracting an angular arm with respect to the x axis coordinate of the rectangular DRA. The evolution of this design is shown in Fig. 7 with its equivalent electric field density for both the rectangular DRA and the trapezoidal DRA. Fig. 7(b) shows the angular cuts that has been made in the rectangular DRA. This angular cut at the edge of the DRA is optimized to match with the designed impedance bandwidth. The side wall with the angular cut is 35 degrees to the normal axis of the DRA. This angular cut was optimized with different angle with impedance bandwidth of the antenna. The antenna performance depends upon the angular cut for generation of dual bandwidth. The permittivity and the quality factor of the DRA remains unchanged by such modification in the shape of the DRA. The dual resonance was generated with ultra-wide impedance bandwidth at θ3 while moving from θ1 to θ3. Using the magnetic wall boundary conditions at the side wall surfaces of dielectric resonator the equations of resonating frequency has been developed. Specific wave numbers are defined as the three-dimensional dielectric resonator has three factors dimension along three coordinate axes, and the wave numbers can be expressed as Kx, Ky and Kz along x, y, and z direction respectively. The DRA height remains unchanged for both the rectangular and the trapezoidal shaped DRA here. As during the design, the angular cut was performed based on the optimization angle with impedance bandwidth without changing the aspect ratio and the quality factor of the antenna. Using the below Eqs. (1) and (2) of wave numbers of a three-dimensional dielectric resonator block, the resonating frequency can be calculated from below mentioned equation. The resonant frequency of a DRA is proportional to ϵ_r^(-1/2), which means wide ranges of permittivity can be used to resonate the antenna at desired frequency bands.

The resonating frequency for a rectangular dielectric resonator can be calculated using (1) and (2).

$$k_x \times tan(k_x d/2) = \sqrt{(\varepsilon_r - 1)k_0^2 - k_x^2} \tag{1}$$

$$\text{where } k_0 = \tfrac{2\pi}{\lambda_0} = \tfrac{2\pi f_0}{c}, \quad k_y = \tfrac{\pi}{a} \quad \text{and} \quad k_z = \tfrac{\pi}{b} \text{ and } k_x^2 + k_y^2 + k_z^2 = \varepsilon_r \times k_0^2 \tag{2}$$

where a, b and d are the physical dimensions of DRA which is proportional to the square root of the dielectric constant of the ceramic-based DRA. Here c is the velocity of light in free space and f_0 is the resonating frequency. Here k indicates the wave number and k_x,k_y and k_z indicates the wave numbers along x,y and z directions respectively. As at the surface of the DRA the tangential component of electric field is zero, it is sown in Eq. (3) as.

$$E_x = 0 \tag{3}$$

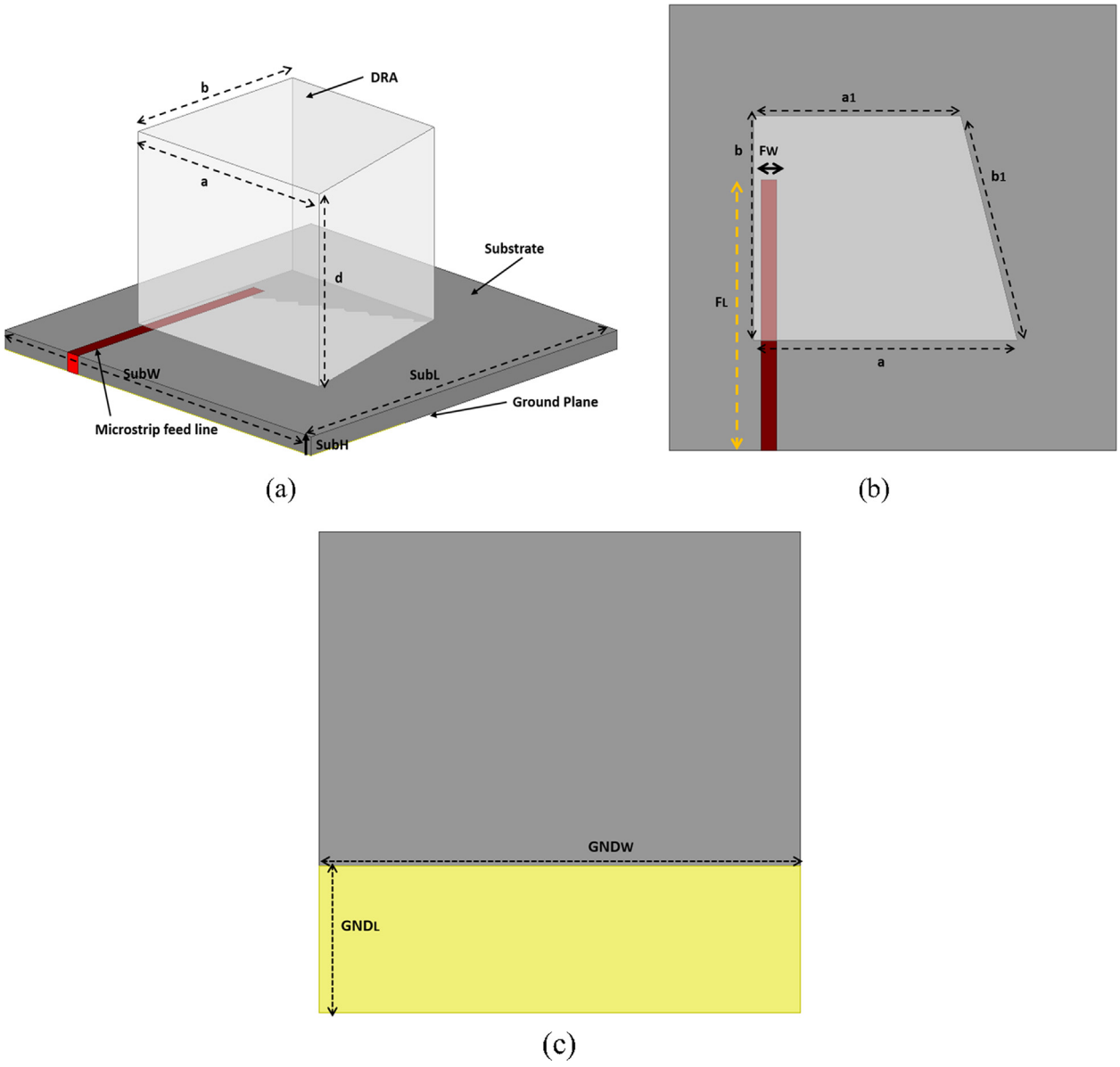

Fig. 3 DRA design (a) DRA fed by a strip line (b) Top view of D R A (c) Bottom view showing the partial ground plane.

As using the phenomena of perfect electric and magnetic fields over the walls of the DRA the following equations represent the distribution of electric fields over the DRA. The DRA is a three-dimensional block representing three different field components of vector electric field. The electric field component along Y and Z direction (Ey and Ez) will be as mentioned in Eqs. (4) and (5).

$$E_Y = Ak_z \cos(k_x x)\sin(k_y y)\sin(k_z z)$$
$$E_z = Ak_y \cos(k_x x)\cos(k_y y)\cos(k_z z) \quad (4)$$

$$E_Y = Ak_z \cos(k_x x)\sin(k_y y)\sin(k_z z)$$
$$E_z = Ak_y \cos(k_x x)\cos(k_y y)\cos(k_z z) \quad (5)$$

The magnetic field across the DRA is represented in convenience with the vector electric field distribution. The DRA electric field volume distribution is as per the mode of excitation and the tangential component of electric and magnetic field which is orthogonal to the electric field is equal to zero at the interface of DRA, which is Z = 0. The following equations of H_x, H_y and H_z shown in Eqs. (6)–(8) represents the magnetic field distribution over the DRA [3].

$$H_x = A\frac{k_Y^2 + k_Z^2}{j\omega\mu_0}\cos(k_x x)\sin(k_y y)\cos(k_z z) \quad (6)$$

$$H_y = -A\frac{k_x k_y}{j\omega\mu_0}\sin(k_x x)\cos(k_y y)\cos(k_z z) \quad (7)$$

$$H_z = A\frac{k_x k_z}{j\omega\mu_0}\sin(k_x x)\sin(k_y y)\sin(k_z z) \quad (8)$$

The calculated DRA dimensions are further optimized to resonate and to achieve a wide impedance bandwidth. The characteristic mode excitation of the DRA is essential to make the DRA more suitable for idle wireless environments. Fig. 7

Table 1 Antenna parameters specifications.

Design Parameters	Parameter Details	Parameter Values In mm
a	DRA Width	3.4
b	DRA Length	2.9
d	DRA Height	2.6
a1	Modified Width	2.66
b1	Modified Length	2.99
Sub_L	Substrate Length	5.76
Sub_w	Substrate Width	5.76
Sub_h	Substrate Height	0.254
F_L	Microstrip Feed Length	5.55
F_W	Microstrip Feed Width	1
GND_L	Ground Length	0.5
GND_W	Ground Width	2

Table 2 Calculated antenna parameters.

Parameter	Parameter Details	Parameter Values
a/d	Aspect ratio	2.07 mm
b/d	Aspect ratio	1.85 mm
Q	Quality factor	35
S_L	Stub length	1.00 mm
εeff	Effective permittivity	2.80
$^{\delta}$Sub	Loss Tangent of Substrate	0.0009
$^{\delta}$DRA	Loss Tangent of DRA	0.002
εSub	Permittivity of Substrate	2.2
εDRA	Permittivity of DRA	10

shows the trapezoidal DRA and a rectangular DRA that are designed at milli meter wave 5G frequency band. The performance of the DRA is investigated. Fig. 8 show the reflection coefficient of both the DRA. The feeding scheme for both the DRA are the same which is microstrip line feeding and it is the edge feeding. The rectangular DRA has generated a multiband with low values of reflection coefficient, but the

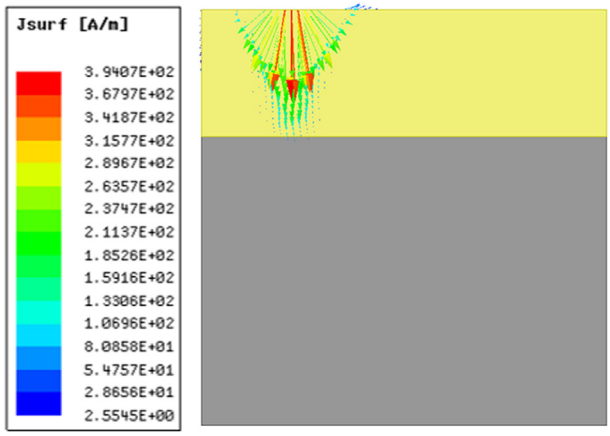

Fig. 5 Surface current over the partial ground plane.

trapezoidal DRA(TDRA) has generated a wide dual band with three different resonances at 22.06 GHz, 24.6 GHz, and 30.42 GHz. Here the trapezoidal DRA has e better reflection coefficient value than that of the rectangular DRA(RDRA). Fig. 9 shows the axial ratio bandwidth of both RDRA and TDRA. Fig. 9 shows the axial ratio behaviour of both DRA. The RDRA is linearly polarized whereas the TDRA is circularly polarized with 3 dB axial ratio bandwidth of 5.46 percentage (24.44–25.86 GHz = 1.42 GHz). The trapezoidal shape formation of the DRA with microstrip edge feeding generates the circular polarization. Fig. 10 shows the gain values of both the RDRA and TDRA. The simulated gain of the RDRA is 1.52 dB and of TDRA is 3.28 dB. The performance of both the RDRA and TDRA are shown in Table 3.

4. Parametric study and analysis

Several parameters have been considered in the optimization study to achieve the maximum impedance bandwidth. The DRA dimensions are calculated as per the desired resonating

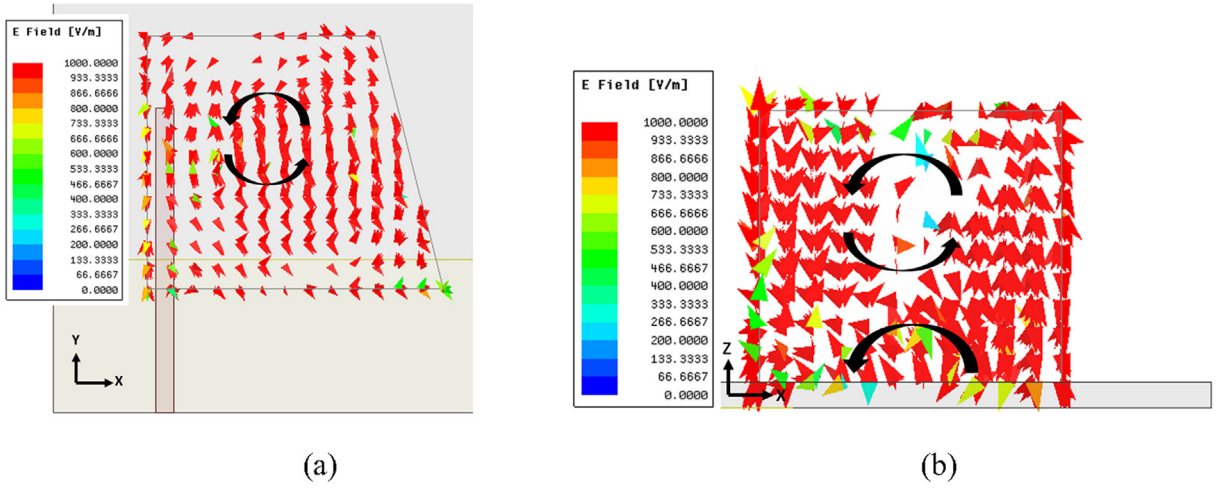

(a) (b)

Fig. 4 Electric field distribution over DRA (a) XY plane (b) YZ plane.

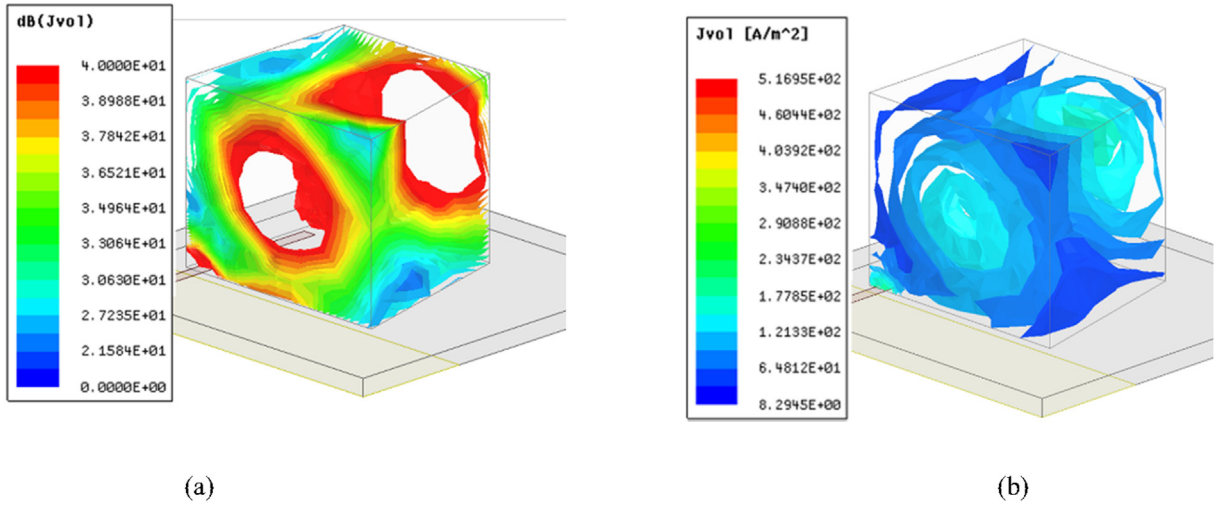

Fig. 6 Electric volume density over the DRA.

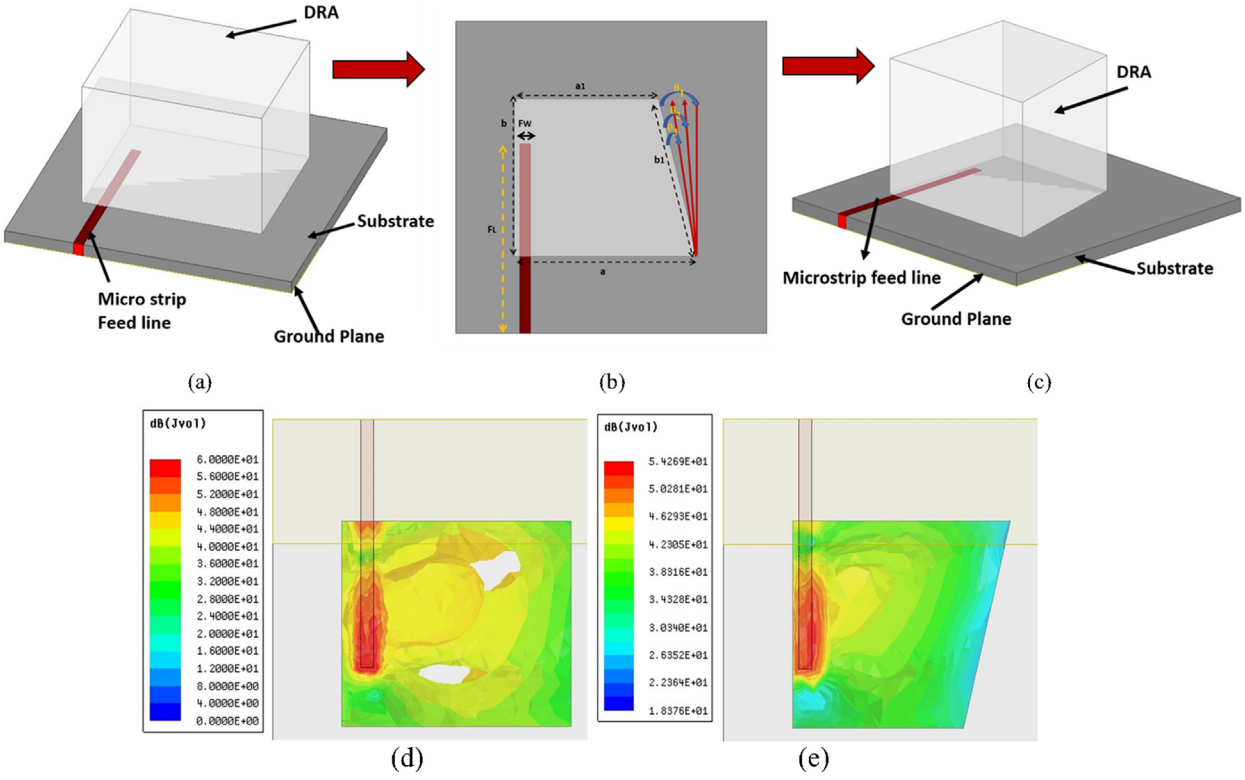

Fig. 7 Evolution of the DRA design (a) Strip line fed Rectangular DRA (b) The angular cut made on the rectangular DRA (c) Strip line fed Trapezoidal DRA, Electric Volume over (d) Rectangular DRA (e) Trapezoidal DRA.

frequency and then are optimized. Here the optimized parameters as DRA height, input impedance of the DRA with varying height of DRA, Axial ratio, and reflection coefficient at different feeding position of microstrip line are considered. Fig. 11 shows the reflection coefficient at different DRA height. The fundamental characteristics mode of excitation changes with the changing DRA dimensions. Fig. 15 represents the input impedance of the DRA at different DRA dimensions. The simulated data of input impedances at different resonances are 70.33 Ohm at 22.06 GHz, 51.54 Ohm at 24.5 GHz and 57.65 Ohm at 29.84 GHz. These impedance values have an idle match with the desired characteristics impedance of the antenna which is 50 Ohm. Fig. 12 shows the corresponding input impedance behavior of the DRA at different height. Fig. 13 shows the axial ratio of DRA at different feed positions. As mentioned earlier the position of the microstrip feeding line is optimized which is shown in Fig. 19 with its 3D radiation pattern. It was started with position 3 and moved

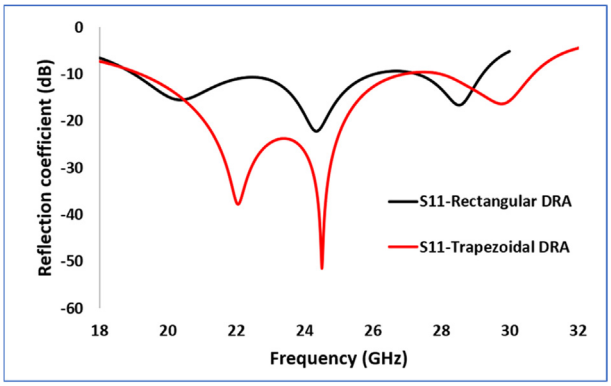

Fig. 8 Reflection coefficient for both DRA.

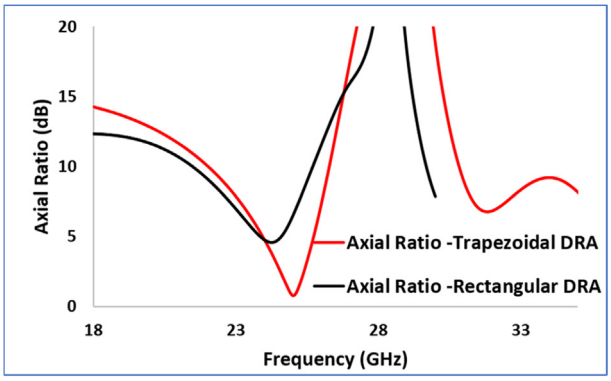

Fig. 9 Axial Ratio of both DRA.

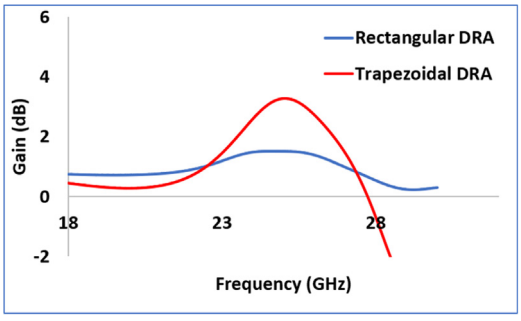

Fig. 10 Gain at different frequencies for both DRA.

Table 3 Performance comparison of both dra.

Antenna Parameters	Rectangular DRA	Trapezoidal DRA
Resonating Frequency (GHz)	20.34 GHz 24.44 GHz 28.56 GHz	22.06 GHz 24.6 GHz 30.42 GHz
Gain (dB)	1.52 dB	3.28 dB
Polarization	Linearly Polarized	Circularly Polarized
Band Type	Multiband	Wide Dual Band

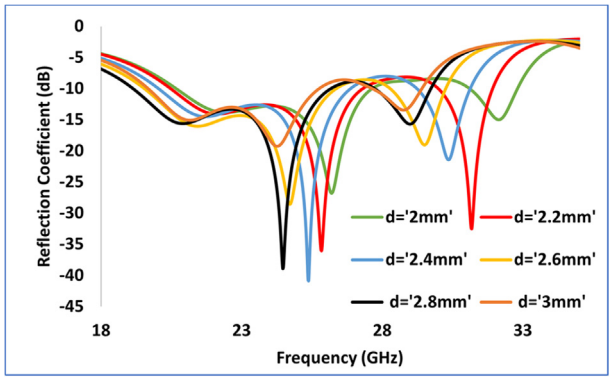

Fig. 11 Reflection coefficient at different DRA height.

to left (position 1) and right (position 5) to get the desired circular polarization bandwidth. So the reflection coefficient of the TDRA at different feed position is shown in Fig. 14. It is the position 1 where better values of reflection coefficient is observed with ultra-wide impedance bandwidth. The desired performance of the TDRA is compared with that of RDRA with many aspects. As rectangular DRA are considered as most conventional antenna, here the trapezoidal DRA has given better results at millimeter wave frequency band applications. These features of wide bandwidth with dual band and circular polarization have many more advantages for millimeter wave 5G applications (see Figs. 16–18).

Fig. 19 shows the microstrip line feeding investigation of TDRA at different positions. The position 1 which is the edge feed is chosen here because of wide bandwidth and circular polarization. The 3D radiation pattern of the TDRA at different positions also shown in Fig. 19. The maximum broadside direction radiation is observed at phi = 0 and theta = 0. All the above radiation has two dip nearly zero radiation field near to theta = 0. Fig. 20 shows the optimization of reflection coefficient at different length of the microstrip feed line. The designed microstrip line feeding is matched with the 50-ohm characteristics impedance. Here the microstrip line feed length is 5.5 mm and feed width are 1 mm. The simulated environments were set with perfect electric field for far field radiation field with satisfied boundary conditions. The DRA exhibits a complex electric field distribution showing its circular field distribution under this edge feeding scheme. Fig. 21 shows the effect of partial ground plane on the DRA design. A roger's substrate of thickness 0.254 mm and 5.76 mm as length and width I used in the antenna design here. The optimization study for partial ground plane effect is done here staring from the full ground plane (5.76 mm) to the partial ground plane (4 mm). The detail ground plane effects on reflection coefficient is shown in Fig. 21 at different resonating frequencies. The partial ground plane effect has also reduced the cross pol radiated power of the DRA. Here the DRA is right hand circularly polarized and has its maximum radiation along the broadside direction. The partial ground plane dimensions are resonated at the desired resonating frequencies and have a low cross pol as shown in Fig. 22. The feeding design scheme as shown in Fig. 15 is experimented considering only the XY plane of reference of the DRA. The DRA is placed on the substrate only in the XY flat surface as the maximum impedance bandwidth was observed. The DRA cut was done as per the

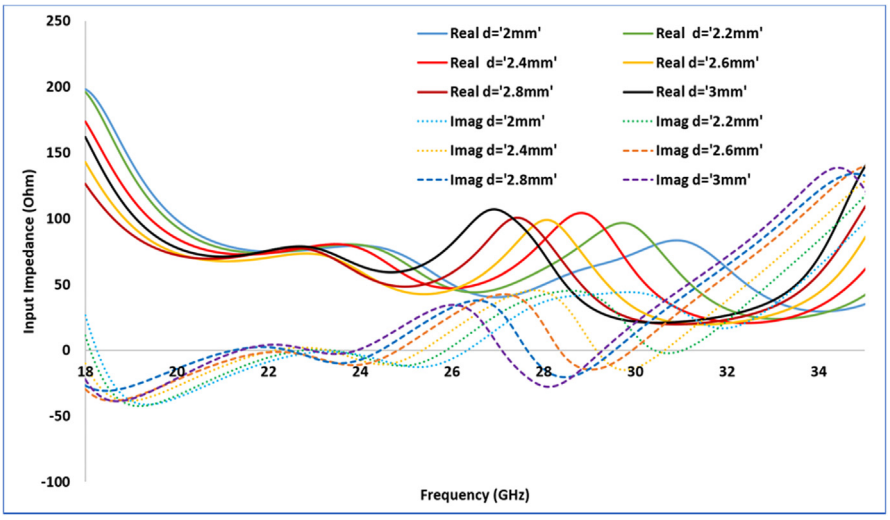

Fig. 12 Input Impedance variation at different DRA height.

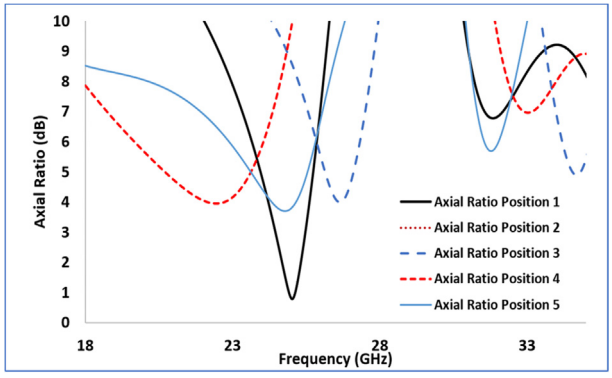

Fig. 13 Axial Ratio at different feed position.

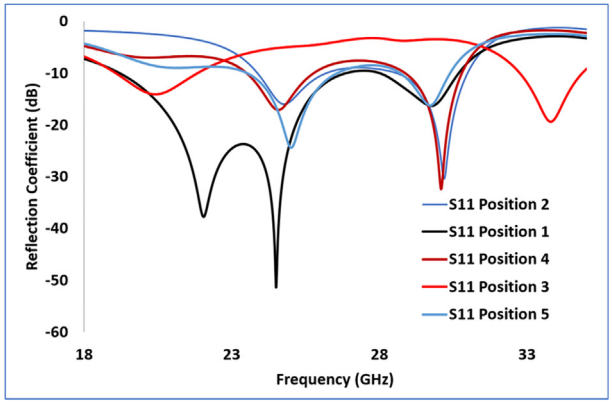

Fig. 14 Reflection coefficient at different feed position.

simulation design of the antenna. The ground plane has been converted from full plane to partial plane and is studied with the matching resonating bandwidth. The excitation of the DRA using a 50-ohm microstrip line at different feed position represents the easy of excitation phenomena with reflection coefficient. The DRA with edge cut has generated the circular polarization and the DRA with the edge feed generate the designed impedance bandwidth.

The feed positions are studied here with respect to the center position of the DRA. The edge feeding which is position 1 has generated circular polarization in the DRA whereas at all other feed positions it is linearly polarized. The details of gain values and polarization at different feed positions are shown in Table 4. The DRA here is right hand circularly polarized (RHCP) and has very low cross pol radiation between 24 GHz and 26 GHz.

5. Results and discussion

The simulated and measured results of reflection coefficient vs frequency is shown in Fig. 22. There is a minimal shift in the frequency with low vales of reflection coefficient in measured results. Both the simulated and measured results have wide dual band in nature. This dual bandwidth is observed in the trapezoidal DRA while compared with the rectangular DRA. The edge cut angular section with an angle of 14 degree is cut from the rectangular DRA. Fig. 22 shows the wide dual band from 19.52 GHz to 26.36 GHz which is 6.84 GHz of bandwidth and band2 from 28.26 GHz to 30.26 GHz which is 2 GHz. There are some dissimilarities between the simulated and measured results of return loss. The simulated reflection coefficient is −37.76 dB and measured reflection coefficient is −16.02 dB at first resonance. At the second resonance the simulated reflection coefficient is −51.46 dB and measured reflection coefficient is −28.56 Db. The third resonance has reflection coefficient of −16.25 dB in simulation and −19 dB in measurement. Fig. 24 shows the simulated and measured gain of the trapezoidal DRA. The DRA designed has gain of 3.8 dB and a variant gain value in measurement as shown in Figure.

The DRA is fixed on the substrate using a conductive glue to strengthen its position on the substrate. The DRA fixing was done manually and because of which some shifting in resonating frequencies and gain vales has been observed here. This fabrication error is because of small size of the DRA and can be adjusted carefully. Here the DRA dimensions are

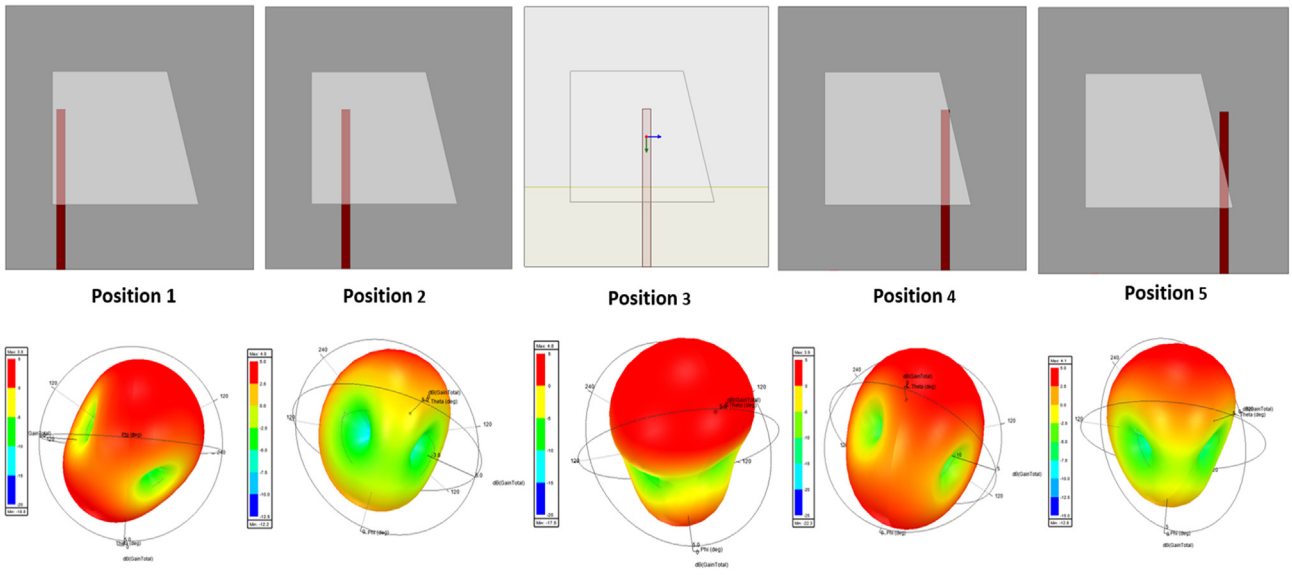

Fig. 15 3D Radiation pattern variation at different feed position.

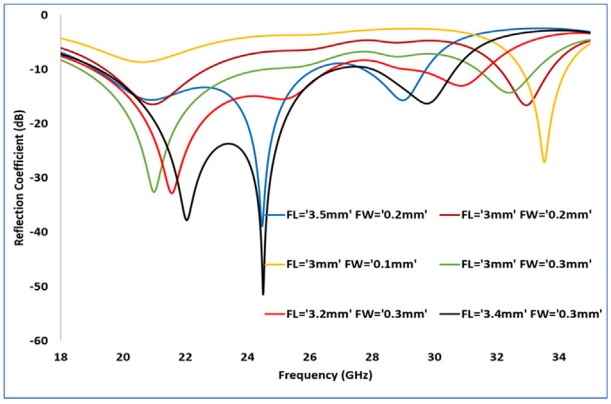

Fig. 16 Reflection coefficient at different feed length.

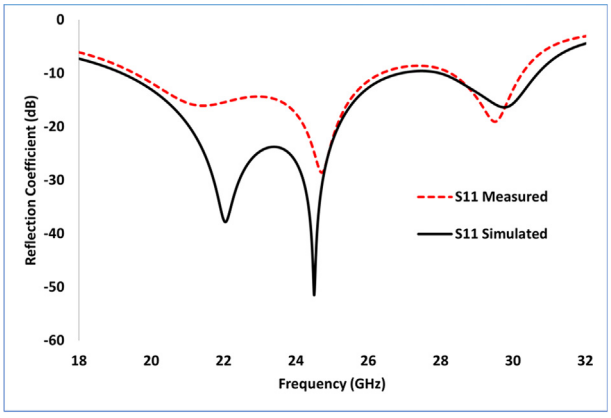

Fig. 18 Reflection coefficient (dB) Vs Frequency (GHz).

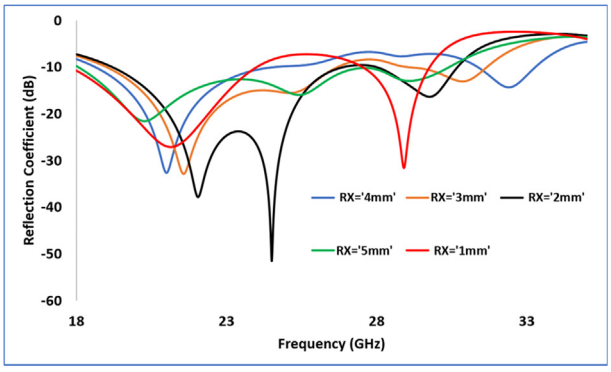

Fig. 17 Reflection coefficient at different ground plane dimensions.

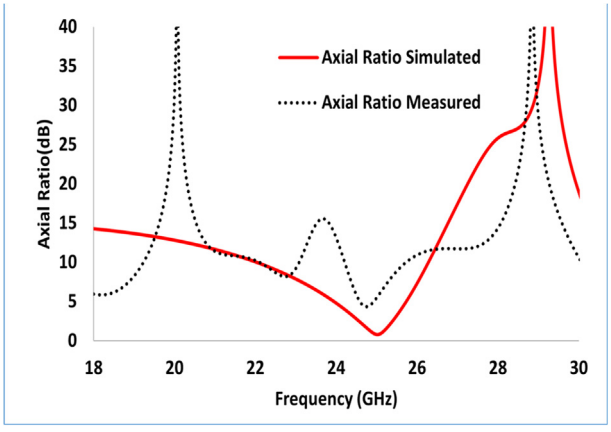

Fig. 19 Axial Ratio (dB) Vs Frequency (GHz).

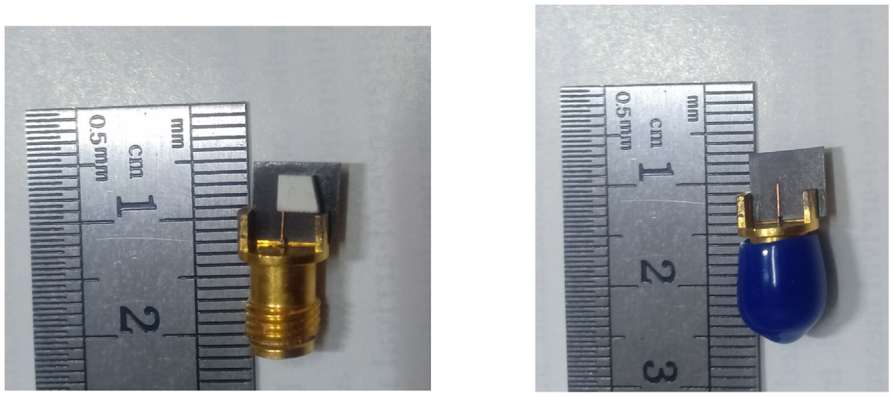

Fig. 20 Fabricated DRA showing (a) Top view (b) Feed Line.

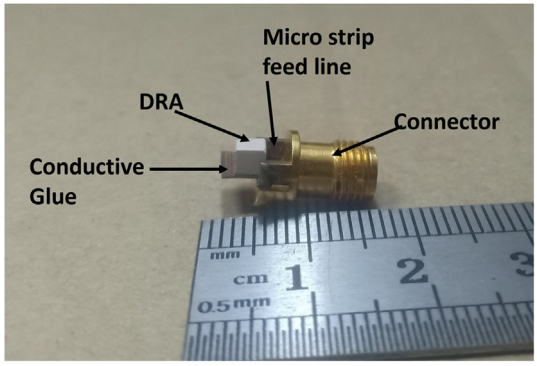

Fig. 21 DRA fabricated unit.

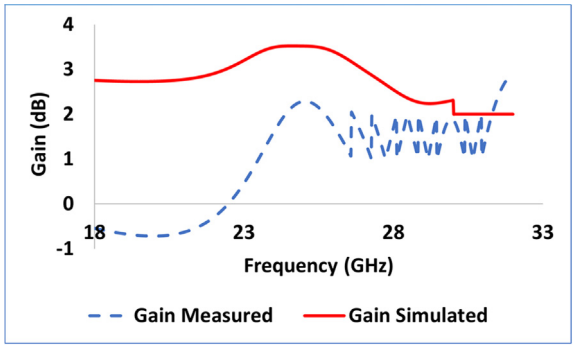

Fig. 22 Gain (dB) Vs Frequency (GHz).

Table 4 Antenna polarization at different feed position.

Antenna Position	Gain (dB)	Polarization
1	3.8	Circular
2	4.0	Linear
3	4.8	Linear
4	3.9	Linear
5	4.1	Linear

3.4 mm × 2.9 mm × 2.6 mm are places over a substrate with dimensions 5.76 mm × 5.76 mm. The fabricated design was measured inside the anechoic chamber considering all the conditions of far field radiation measurements. A 40 GHz horn was used to measure the radiation pattern of the DRA. Fig. 23 shows the fabricated units of the DRA with substrate and connector. The DRA has three resonating frequencies as 22.06 GHz, 24.5 GHz and 29.84 GHz. The DRA has impedances of 70.33 Ohm at 22.04 GHz, 51.54 Ohm at 24.5 GHz and 57.65 Ohm at 29.84 GHz respectively. These input impedances vary with the source to connector voltages. The DRA also has achieved gain of 3.98 dB in simulation and 2.79 dB

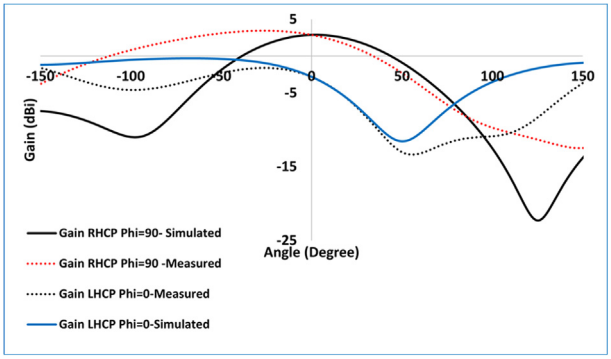

Fig. 23 Radiation Pattern at 22.06 GHz.

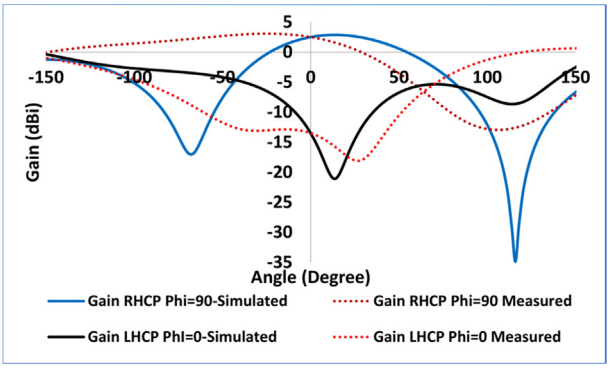

Fig. 24 Radiation Pattern at 24.5 GHz.

in measurement at 22.06 GHz, 2.62 dB in simulation and 2.28 dB in measurement at 24.5 GHz and 2.41 dB in simulation and 1.33 dB in measurement at 29.84 GHz. The connector to antenna load impedances depends on the fabrication process as here the DRA is very small in size. The DRA placement over the substrate was also done manually. These have been challenging as many displacements has been seen in the antenna performances. These displacements also change the resonating frequency shift. The DRA is fixed over the substrate using a conductive glue.

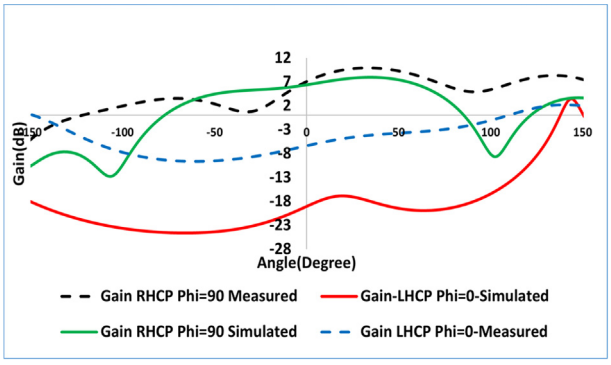

Fig. 25 Radiation Pattern at 29.84 GHz.

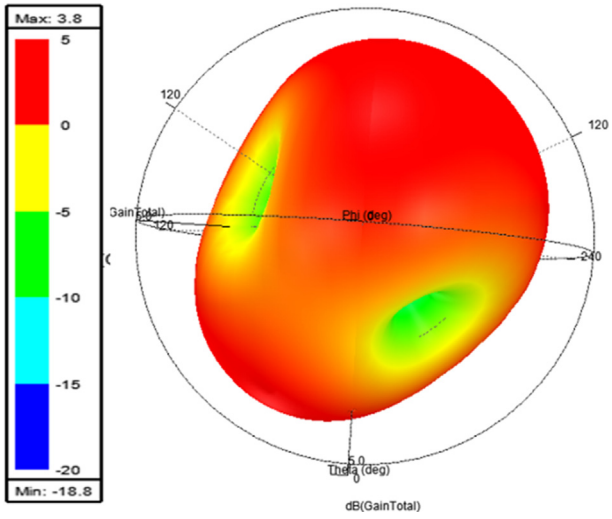

Fig. 26 3D Radiation pattern of DRA.

The radiation pattern for both E and H plane show in Fig. 23, Fig. 24 and Fig. 25 at 22.06 GHz, 24.5 GHz, 29.84 GHz respectively. The DRA here is right hand circularly polarized and has maximum direction of radiation towards the broadside direction. Fig. 26 shows the three-dimensional radiation pattern of the antenna which has two minima near to zero radiation points. The comparison of several DRA shapes is studied here and is compared with the novel trapezoidal shape DRA, which is shown in Table 5. The selection of different DRA shapes is done at millimeter wave frequencies only as the DRA elements have the nearly similar values of permittivity. The proposed trapezoidal shaped DRA has achieved higher impedance bandwidth of 26.3% and 7.69% with dual band generation. The antenna is circularly polarized and has achieved a gain value of 3.98 dBi. The permittivity of 10 generally generates a ultra-wide bandwidth at millimeter wave frequencies. Several DRA shapes are studied over last decade but most popular and conventional DRA shapes are chosen here to compare the antenna performances. The measurement setup of the antenna is shown in Figs. 27 and 28. The radiation pattern measurement was carried out inside the anechoic chamber using a 40 GHz horn antenna as a receiver. The polarization of electric field was observed as per the broadside direction. Minimum cross polarization was observed at 24.5 GHz during the

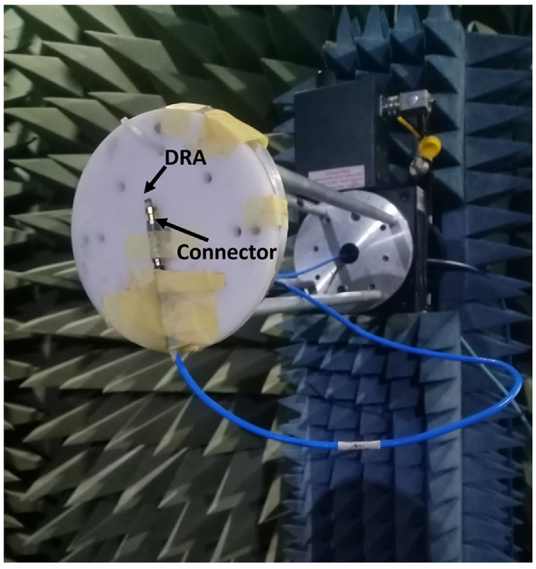

Fig. 27 Antenna Measurement inside anechoic chamber.

Table 5 Antenna performance comparison.

Ref. No.	DRA Shape	Permittivity	Frequency (GHz)	Feed Type	DRA Dimensions (mm × mm × mm)	Bandwidth (%)	Gain (dB)
[15]	Rectangular	10	26 GHz	Microstrip line	2.9 × 2.9 × 1.4	4.3%	8.04
[16]	Rectangular	10	26 GHz	Microstrip line	2.9 × 2.6 × 1.4	20.15%	6.3
[17]	Elliptical	10.2	60 GHz	Aperture Coupled	6.6 × 7.2 × 0.63	12 %	9
[18]	Rectangular	10	24 GHz	Aperture Coupled	4.8 × 6.4 × 3	3.87%	6.2
[19]	Cylindrical	10.2	60 GHz	Substrate Integrated	0.65 × 0.15	9.33%	7.15
[20]	Rectangular	9.8	28 GHz	Aperture Coupled	9.5 × 7.5 × 2.54	4.78%	12
Proposed	Trapezoidal	10	26 GHz	Microstrip line	2.9 × 3.4 × 2.6	26.3% & 7.69% (Dual Band)	3.98

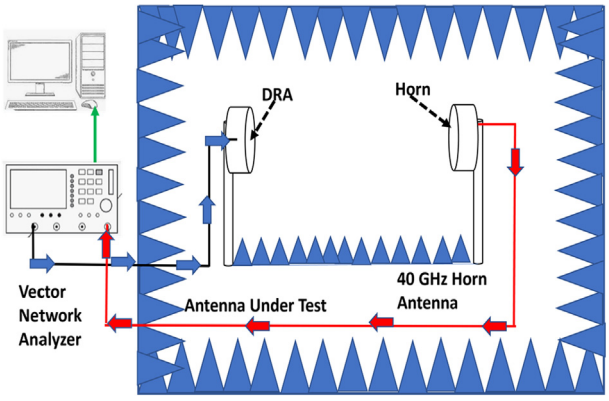

Fig. 28 Antenna Measurement setup.

Table 6 Antenna gain results.

Frequency (GHz)	Gain (dB)	Antenna Impedances/ Reactance
22.06	3.98 (Simulated)	70.33
	2.79 (Measured)	−1.4
24.5	2.62 (Simulated)	51.54
	2.28 (Measured)	−7.3
29.84	2.41 (Simulated)	57.65
	1.33 (Measured)	−14.02

measurement of the antenna. The distance observed between the transmitter and receiver antenna was 1.5 m as DRA is very small in size.

5.1. Measurement of gain and efficiency: Critical issues

A coaxial cable was used as the antenna feeder which was fixed on a plastic mounting plate facing towards the receiver. The cable losses were observed during the calibration of receiver antenna gain. The far field observation point was fixed at 1.7 m for the measurement of radiation pattern. The antenna feeder cable was connected to the vector network analyzer as shown in Fig. 28.

The gain value of the antenna while simulation and measurement is shown in Table 6. There were few uncertainties in gain values due to.

1. Cable losses in the antenna feeder.
2. Fabrication errors as the DRA was fixed using a conductive glue on the substrate.

The gain and efficiency measurement of DRA at millimeter wave frequencies depends upon the radiated Q factor of the antenna. As here we have used a higher permittivity value Of DRA for wider impedance bandwidth.

6. Conclusions

A wide dual band circularly polarized DRA has been designed here for millimeter wave 5G frequency bands is resonating at 22.06 GHz, 24.5 GHz, and 29.84 GHz which is 26.3 percentage of impedance bandwidth at first band and 7.69 percentage at second band. The DRA is right hand circularly polarized and has got 3-dB polarization bandwidth of 5.23 percentage. This microstrip feed line DRA has covered the complete bandwidth from 19.52 GHz to 26.36 GHz and 28.26–30.26 GHz covering all the frequency bands of 5G below 30 GHz at millimeter wave. This work can further be used in making larger arrays for indoor small cells for wideband applications.

Declaration of Competing Interest

The authors declare that they have no known competing financial interests or personal relationships that could have appeared to influence the work reported in this paper.

Acknowledgement

This work was supported by Universiti Teknologi Malaysia under TDR grant vote 05G20 and HiCOE grant vote 4J415.

References

[1] A. Petosa, A. Ittipiboon, Dielectric Resonator Antennas : A Historical Review and the Current State of the Art, 52(5) (2010).
[2] D. Lee, A. Petosa, D. Guha, Y.M.M. Antar, A. Ittipiboon, Improved Design Guidelines for the Ultra Wideband Monopole-Dielectric Resonator Antenna, IEEE Antennas Wirel. Propag. Lett. 5 (2006) 373–376, https://doi.org/10.1109/lawp.2006.881922.
[3] R.K. Mongia, A. Ittipiboon, Theoretical and Experimental Investigations on Rectangular Dielectric Resonator Antennas, 45(9) (1997) 1348–1356.
[4] R.K. Mongia, P. Bhartia, Dielectric resonator antennas—a review and general design relations for resonant frequency and bandwidth, Int. J. Microw. Mill.-Wave Comput.-Aided Eng. 4 (3) (1994) 230–247.
[5] D.-W.C. D. Resonator, Linear-/Circular-Polarization Designs of, IEEE Trans. Antennas Propag., 60(6) (2012) 2662–2671, doi: 10.1109/TAP.2012.2194682.
[6] A.A. Kishk, Wide-Band Truncated Tetrahedron Dielectric Resonator Antenna Excited by a Coaxial Probe, IEEE Trans. Antennas Propag. 51 (10) (2003) 2913–2917, https://doi.org/10.1109/TAP.2003.816300.
[7] A. Gaya, I. Ali, Performance Analysis of a Dielectric Resonator Antenna with Different Feeding Technique for 5G Communication, in: 2018 2nd International Conference on Electrical Engineering and Informatics (ICon EEI), (2018), no. October, pp. 92–97.
[8] Z. Song, H. Zheng, M. Wang, Y. Li, T. Song, E. Li, Y. Li, Equilateral Triangular Dielectric Resonator and Metal Patch Hybrid Antenna for UWB Application, IEEE Access 7 (2019) 119060–119068.
[9] M. Zou, J. Pan, Wide Dual-Band Circularly Polarized Stacked Rectangular Dielectric Resonator Antenna, IEEE Antennas Wirel. Propag. Lett. 15 (2016) 1140–1143, https://doi.org/10.1109/LAWP.2015.2496361.
[10] A. Gaya, M.H. Jamaluddin, Wideband Aperture coupled Rectangular Dielectric Resonator Antenna for mm wave 5G Applications, in: 2019 8th Asia-Pacific Conference on Antennas and Propagation (APCAP), (2019), pp. 442–443, doi: 10.1109/APCAP47827.2019.9472034.
[11] A. Gaya, M.H. Jamaluddin, A. Abdulhadi Althuwayb, Wideband Circularly Polarized Millimeter Wave Dielectric Resonator Antenna with defected ground structure for 5G Communications, in: (2020) IEEE MTT-S Int. Conf. Numer.

Electromagn. Multiphysics Model. Optim. NEMO 2020, doi: 10.1109/NEMO49486.2020.9343497.
[12] S. Keyrouz, D. Caratelli, Dielectric Resonator Antennas: Basic Concepts, Design Guidelines, and Recent Developments at Millimeter-Wave Frequencies, Int. J. Antennas Propag. 2016 (2016) 1–20, https://doi.org/10.1155/2016/6075680.
[13] R.K. Mongia, A. Atipiboon, M. Cuhaci, D. Roscoe, Radiation Q-factor of rectangular dielectric resonator antennas: theory and experiment, Int. IEEE APS Symp. (2009) 764–767.
[14] C.A. Balanis, Antenna Theroy: Analysis and Design, 3rd ed., Wiley, 2012.
[15] A. Gaya, M.H. Jamaluddin, I. Ali Althuwayb, Circular Patch Fed Rectangular Dielectric Resonator Antenna, Sensors (Switzerland) (2021), https://doi.org/10.3390/s21082694.
[16] Aayesha, M. Bilal Qureshi, M. Afzaal, M. Shuaib Qureshi, J. Gwak, Ultra-Wideband Annular Ring Fed Rectangular Dielectric Resonator Antenna for Millimeter Wave 5G Applications, CMC-Comput. Mater. Continua 71 (1) (2022) 1331–1348.
[17] A. Perron, S. Member, T.A. Denidni, S. Member, A.R. Sebak, Circularly Polarized Microstrip/Elliptical Dielectric Applications, 9 (2010) 783–786.
[18] Y.-M. Pan, K.W. Leung, K.-M. Luk, Design of the Millimeter-wave Rectangular Dielectric Resonator Antenna Using a Higher-Order Mode, IEEE Trans. Antennas Propagat. 59 (8) (2011) 2780–2788.
[19] Y.-X. Sun, K.W. Leung, Circularly Polarized Substrate-Integrated Cylindrical Dielectric Resonator Antenna Array for 60 GHz Applications, Antennas Wirel. Propag. Lett. 17 (8) (2018) 1401–1405.
[20] Y. Zhang, J.-Y. Deng, M.-J. Li, D. Sun, L.-X. Guo, A MIMO Dielectric Resonator Antenna With Improved Isolation for 5G mm-Wave Applications, Antennas Wirel. Propag. Lett. 18 (4) (2019) 747–751.